Optical Engineering

SPIEDigitalLibrary.org/oe

Long-stroke fast tool servo and a tool setting method for freeform optics fabrication

Qiang Liu
Xiaoqin Zhou
Zhiwei Liu
Chao Lin
Long Ma

Long-stroke fast tool servo and a tool setting method for freeform optics fabrication

Qiang Liu,[a] Xiaoqin Zhou,[a,*] Zhiwei Liu,[a] Chao Lin,[b] and Long Ma[a]
[a]Jilin University, School of Mechanical Science and Engineering, Changchun 0086130025, China
[b]Chinese Academic of Sciences, Changchun Institute of Optics, Fine Mechanics and Physics, Space Optics Research Laboratory, Changchun 0086130033, China

Abstract. Diamond turning assisted by fast tool servo is of high efficiency for the fabrication of freeform optics. This paper describes a long-stroke fast tool servo to obtain a large-amplitude tool motion. It has the advantage of low cost and higher stiffness and natural frequency than other flexure-based long-stroke fast tool servo systems. The fast tool servo is actuated by a voice coil motor and guided by a flexure-hinge structure. Open-loop and close-loop control tests are conducted on the testing platform. While fast tool servo system is an additional motion axis for a diamond turning machine, a tool center adjustment method is described to confirm tool center position in the machine tool coordinate system when the fast tool servo system is fixed on the diamond turning machine. Last, a sinusoidal surface is machined and the results demonstrate that the tool adjustment method is efficient and precise for a flexure-based fast tool servo system, and the fast tool servo system works well on the fabrication of freeform optics. [DOI: 10.1117/1.OE.53.9.092005]

Keywords: diamond turning; fast tool servo; freeform optics; tool centering adjustment.

Paper 140091SS received Jan. 18, 2014; revised manuscript received Mar. 18, 2014; accepted for publication Mar. 19, 2014; published online Apr. 28, 2014.

1 Introduction

Freeform optics have extensively received increasing requirements in aerospace, national defense, and consumer-oriented industries due to their superior advantages, such as optimum optical performances, miniaturized configurations, etc.[1–5] Because of the complex surface shapes, it is difficult to fabricate freeform surfaces with optical quality. How to fabricate freeform optical surfaces with high frequency and low cost has attracted an enormous amount of attention in both academic and engineering circles. One of the most flexible ways to fabricate this kind of surface is single-point diamond turning assisted by fast tool servo (FTS). The working principle is explained in Fig. 1. FTS is mounted on a diamond turning machine (DTM), which can move along x direction and z direction, and the workpiece is clamped on the spindle. FTS can translate diamond tool in and out of the workpiece several times per revolution to obtain a freeform surface.

In 1980s, Patterson and Magreb in Lawrence Livermore National Laboratory designed a micro-feed system for error compensation, and the concept of FTS was first introduced.[6] Then, Massachusetts Institute of Technology, Bremen University, Tohoku University, and many other units have devoted resources to developing FTS technology. An FTS system is an independent closed-loop working system mainly consisting of an FTS device and controller. Guide mechanism, actuator, and displacement sensor are key elements of an FTS device, which has attracted most of the attention, and various devices have been developed with a wide variety of mechanical structures and different types of actuators. High-performance controllers and trajectory tracking control algorithms are needed to control the FTS device to obtain high precision, high bandwidth, and high motion resolution. Otherwise, the toolpath for given freeform surfaces and machining parameters must be calculated and optimized. Obviously, the first step to fabricate a freeform optical surface by FTS diamond turning is that an FTS system must be developed and be fixed on DTM. However, FTSs serve as an additional motion axis of the DTM. The tool center position in the machine tool coordinate system should be confirmed while FTS is fixed on the DTM. Based on this, this paper intends to design a low-cost and high-precision long-stroke FTS system and introduce a simple precision tool center position adjusting method.

The main differences of FTS systems are the actuator and mechanical structure. According to the working principle of actuators, FTSs are mainly actuated by piezoelectric actuators and Lorenz force–based motors. FTSs can also be categorized according to their operating range, frequency, and motion mode, and short stroke is defined as <100 μm, intermediate as between 100 μm and 1 mm, and long stroke as >1 mm.[7] Flexure hinge structures and air bearing are designed as the guide mechanisms, where air bearing is mainly for long-stroke FTSs.

Most FTSs are actuated by piezoelectric actuators with high working frequency, the strokes of which are generally <100 μm. Kim et al. designed a flexure-based FTS with a stacked-type piezoelectric actuator to compensate in real time for the thermal growth spindle error. This FTS can move several micrometers in z-direction with motion resolution of 0.15 μm, which is capable of fabricating aluminum mirrors 100 mm in diameter to a form accuracy of 0.1 μm in terms of peak-to-valley (PV) error value.[8] Gan et al. used a piezoelectric actuator–based FTS to compensate for the global straightness error of the translational slide. The error was measured and compensated for in real time. A proportion-integration (PI) feedback controller was implemented

*Address all correspondence to: Xiaoqin Zhou, E-mail: xqzhou@jlu.edu.cn

0091-3286/2014/$25.00 © 2014 SPIE

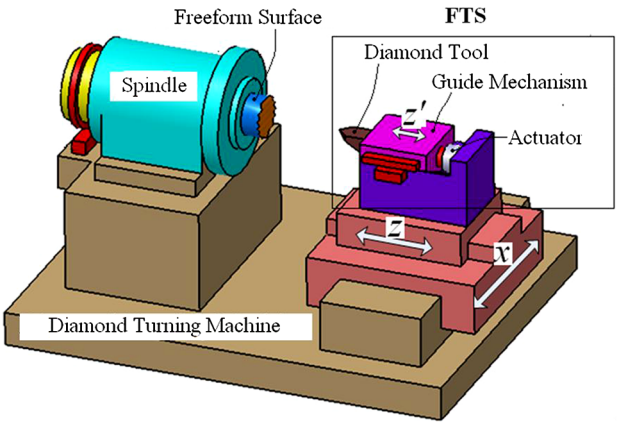

Fig. 1 Working principle of fast tool servo (FTS)-assisted diamond turning.

for better tracking performance. The PV waviness was reduced to 0.18 from 0.9 μm.[9] Kim et al. designed an FTS to fabricate freeform optical surfaces. In order to obtain a longer stroke, lever structure–based mechanisms were implemented in the piezoelectric actuated FTS, which obtained a 432-μm working stroke.[10] However, it significantly increased the FTS system dimension and the number of the motion components, consequently bringing down the bandwidth and stability of the cutting system. Obviously, because of the limited working stroke, piezoelectric actuators–based FTS are more suitable to compensate for motion errors of machine tool or fabricate microstructured surfaces and small-amplitude freeform surfaces.

Since several hundred micrometer- or millimeter-level strokes are needed to fabricate freeform optical surfaces, the Lorenz force–based actuating approach is a fine choice for long-stroke FTS, which can be categorized into three types, namely rotary motors, linear motors, and voice coil motors (VCM). Ludwick[11] and Chargin[12] designed a rotary motor actuated FTS in their PhD theses. The working accuracy was ~1 μm, which was considered very high at that time; the performance can be improved by the better bearing and controller. However, there are some difficulties in the tool path generation for the rotary FTS; fewer researchers paid attention to this type of FTS after that. Nathan designed a linear motor actuated FTS in his master degree thesis. But the working frequency was limited by the heating problem of motor coil.[7] VCMs, which can obtain a higher operating frequency than the linear motors, have been regarded as a very promising choice for the actuation of long-stroke linear FTSs. Zdanowicz designed an FTS with VCM and air bearing. Two smaller VCM actuated mass cancellation structures have been developed to offset the inertia force of VCM coil and air bearing. The working frequency is 20 Hz when the working stroke is $\pm$2 mm.[13] Byl designed a VCM and an air bearing for his long-stroke FTS. The linear FTS has a travel range of 25 mm and is capable of 100 m/s^2 accelerations. The FTS is attached to a hydrostatic bearing supported in feed stage, which is allowed to move in response to the FTS actuation forces and, thus, acts as an integral balance mass.[14] Precitech[15] and Moore Nanotechnology[16] developed several FTSs with air bearing and VCMs, but no reports have been found to introduce the detailed structures. Scheiding et al. used NFTS-6000 from Moore Nanotechnology Systems to fabricate a micro optical lens array on a steep curved substrate with measured shape error of 1.37 μm (rms).[17] Rakuff and Cuttino designed a flexure-based long-stroke FTS with VCM. The maximum stroke is 2 mm. The working frequency is ~80 Hz when working stroke is 280 μm. Different damping materials have been studied to improve the working performance.[18] However, the resonance frequency is brought down by low stiffness of the flexure hinge, which is to obtain a long stroke. The second-order resonance frequency is ~38 Hz. Noh et al. designed a VCM and a disc spring for a new FTS to fabricate a micro-lens. The bandwidth is 273 Hz and z-direction stiffness is 0.21 N/μm.[19]

As mentioned above, long-stroke FTSs are needed to fabricate freeform optical surfaces, and VCM is the best choice as the actuator. Most long-stroke FTSs are guided by air bearings. However, an additional air supply system is needed. With large moving mass of air bearing and high working frequency, a damper must be designed to eliminate the inertia force; otherwise the inertia force may greatly bring down the FTS working performance. Besides, the high-precision air bearing is difficult to fabricate. Flexure hinges are extensively used in micro-displacement systems. They have the advantages of no backlash, high precision, and low cost. In FTS system, the flexure hinge needs to withstand the alternating cutting force, and large deformation will bring down the stiffness to generate machining errors. Long stroke and high stiffness are two mutual constraint elements of flexure hinges limiting the application in long-stroke FTS.

In this research, a cross-shape flexure hinge structure with high stiffness is designed and a VCM is selected to develop a long-stroke FTS. The design calculation is thoroughly described, and off-line performances are tested on an isolation platform. Few reports have introduced tool centering adjustment methods when FTS is fixed on DTM. An easy and precise method is described. Last, a typical freeform surface has been machined to verify the tool setting method and FTS cutting performance.

2 Long-Stroke FTS System Design

A BEI Kimco VCM is chosen as the driving element. This actuator with diameter of 69.85 mm provides maximum continuous stall forces of 82.74 N and short-term peak forces of 266.89 N. The displacement of FTS is measured by a Renishaw linear encoder with resolution of 0.01 μm. The read head is installed on the base and the scale is pasted on the moving part of the FTS. Cross-shape flexure hinges providing high stiffness in the x and y directions are designed to guide tool motion.

The parameters of the cross-shape hinge are shown in Fig. 2. The stiffness in z direction K_z can be calculated as follows:

$$K_z = \frac{F}{z} = \frac{4Ebh^3}{l^3}. \tag{1}$$

The flexure hinge stiffness in x and y direction is

$$K_{x,y} = \frac{2Ebh^3}{l^3} + 2 \cdot \frac{EA}{l}, \tag{2}$$

where $A = b \bullet h$ is the cross-sectional area of the flexure hinge. The parameter values and calculation results are

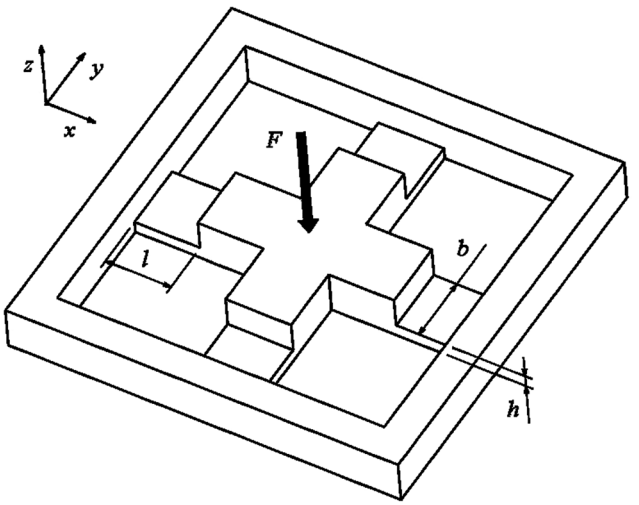

Fig. 2 The cross-shape hinge structure.

shown in Table 1. It can be seen that the x and y direction stiffness values of the flexure hinge are far higher than z direction stiffness.

Another characteristic of the chosen VCM used in this research is that there is a through hole with diameter of ~12.7 mm in the VCM stator as shown in Fig. 3. Two cross-shape flexure hinges can be connected by a linking member across the VCM stator. The FTS system details are shown in Fig. 4 and the working principle is explained in Fig. 5.

The linking member with diameter of 12 mm can be considered to be a rigid body. The simplified schematic diagram of the FTS flexure structure is described in Fig. 6. With high stiffness in x and y direction of the cross-shape flexure hinge, the applied force on diamond tool in xy plane $F_{x,y}$, including cutting force and other disturbance forces, can be neglected, while F_z can be compensated by closed-loop control. Little buckling distortion is generated in this structure. Most of the moving mass distributes between the two fulcrums. Therefore, this structure ensures that FTS can keep stabilization and high precision during the machining process even when there are some disturbances.

Mechanical resonance frequency f of the FTS is expressed as

$$f = \frac{1}{2\pi}\sqrt{\frac{k}{m}}, \tag{3}$$

where m is the FTS moving parts mass, which is ~443 g. While the FTS system is guided by two flexure hinges, z direction stiffness of the FTS k is $2 \bullet K_z$. The moving part contains the motor coil, the linking member, tool holder, bolts, and the flexure hinges, which is calculated by computor aided tridimonsional intorface application. Using the

Table 1 Parameter values of the flexure hinge.

l	b	h	E	K_z	$K_{x,y}$
22 mm	12 mm	0.5 mm	190 GPa	107.6 N • mm^{-1}	134.4 × 10^3 N • mm^{-1}

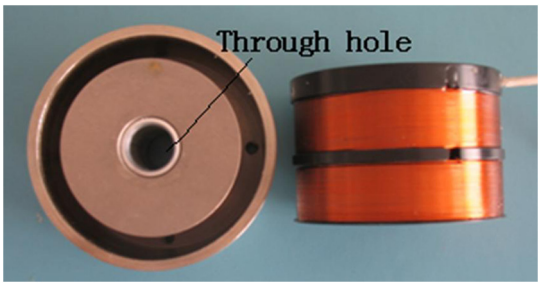

Fig. 3 The chosen voice coil motors of the FTS.

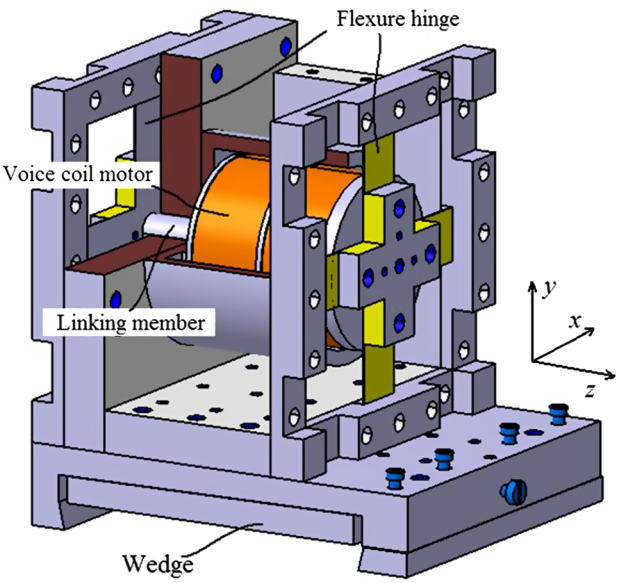

Fig. 4 The details of the FTS.

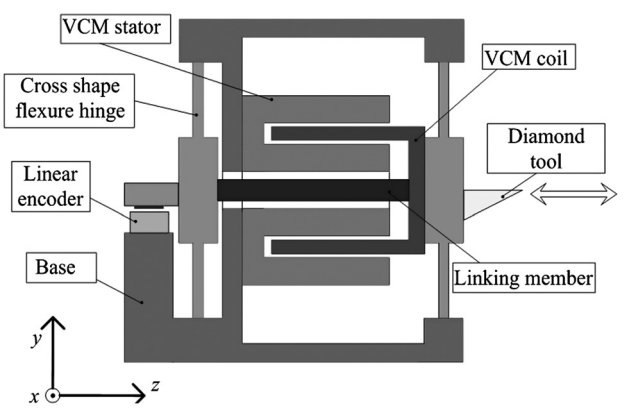

Fig. 5 The designed FTS system working principle.

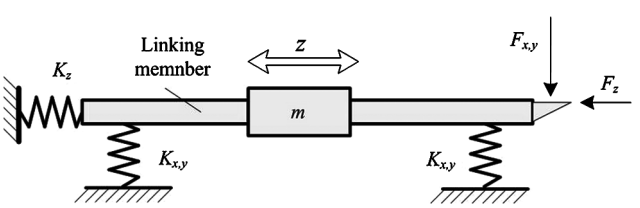

Fig. 6 The simplified schematic diagram of the FTS flexure structure.

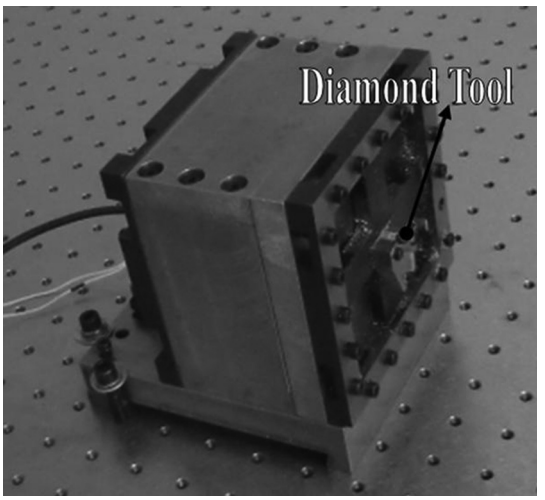

Fig. 7 The photo of flexure hinge based long stroke FTS.

theoretical stiffness and mass, the resonance frequency of the FTS is ~110.98 Hz.

3 Off-Line Testing Results and Discussion

To reduce the environment disturbance, the experiments are carried out on the Newport RS4000 vibration-isolated optical table. The resolution of the D/A converter is 16 bit. The environment noise level is ~8 nm. Figure 7 shows the photo of FTS fixed on the test-bed.

3.1 *Open-Loop Test*

The stiffness of the FTS is tested first. FTS system is bolted horizontally on the optical table, and calibrated weights are applied to the flexure hinge in the z direction. The displacement is recorded by the linear encoder. Then, the stiffness of the FTS in the z direction is obtained. The experiment value is ~105.2 $\mathrm{N\,mm^{-1}}$, which is smaller than the theoretical value. The idealization of theoretical calculation formula, the differences of material natural parameters, machining errors of the cross-shaped flexure hinge, the measurement accuracy and so on, all these elements generate deviation between the actual value and the theoretical value. But, the flexure hinge stiffness in z direction is not the key factor of FTS system, which influences the maximum working stroke and resonance frequency. Small amount of deviation has little effect on FTS working performance.

The open-loop test was carried out, and the result is shown in Fig. 8. The damping coefficient of the structure is determined by the following equation:

$$D = 2\xi\sqrt{K \cdot m}, \tag{4}$$

where ξ is the damping ratio, which is given by $\xi = 1/[2j\pi \ln(x_i/x_{i+j})]$; x_i and x_j is the amplitude from the impact response curve. So, the damping coefficient of the large stroke flexure is 30.48 $\mathrm{N \cdot s \cdot m^{-1}}$. This value influences the stabilization time and overshoot of FTS system, and further influences the response frequency and tool positioning accuracy, and it can be improved by the controller or a damping structure. In this research, the experimental method is implemented to adjust the proportional, integral, and derivative (PID) parameters, which the damping

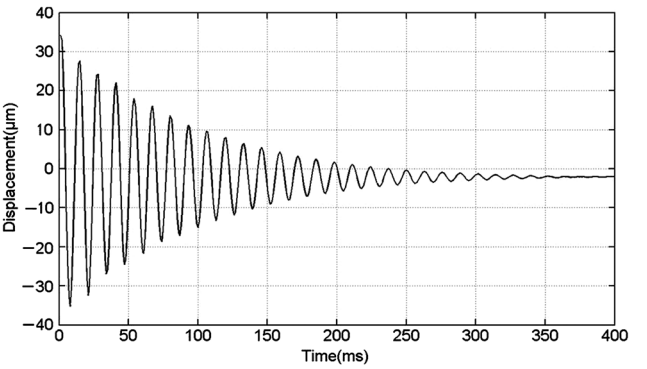

Fig. 8 The open-loop response of the new FTS.

performance is simultaneously improved. The first-order resonance frequency is ~106.6 Hz obtained from the FFT of the impact response, as shown in Fig. 9. Resonance frequency is the harmful element in FTS diamond turning, bringing machining error—even destruction—to the workpiece. Otherwise, FTS working frequency is a continuously changing value in the cutting process, which is decided by the freeform surface geometry and spindle speed. Therefore, FTS must work below the first resonance frequency to avoid resonance vibration during cutting process. It means that the system first resonance frequency is the key influencing factor of FTS working bandwidth.

3.2 *Closed-Loop Test*

A simple PID controller is implemented to control the long-stroke FTS. Closed-loop experiments are carried out to verify the performance of the FTS system. With amplitude of 1 mm, tool working frequency is ~30 Hz, and the amplifier of VCM will generate a good deal of heat as the frequency increases. Another high-performance VCM amplifier is needed to increase tool working frequency.

The resolution is the main target for the design of FTSs. It is the minimum motion step length influencing the trajectory tracking accuracy. The lower the motion revolution, the higher the trajectory tracking accuracy and the higher the machining accuracy. In theory, the flexures of this FTS can obtain a resolution of 5 nm.[18] But some factors may bring down the resolution, such as the resolution of the feedback

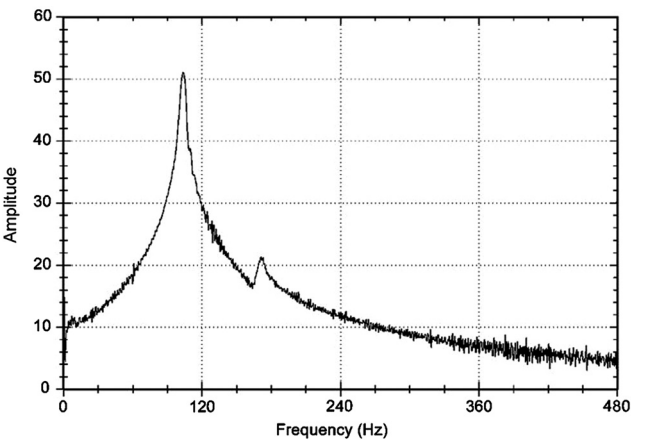

Fig. 9 The FFT of the open-loop response.

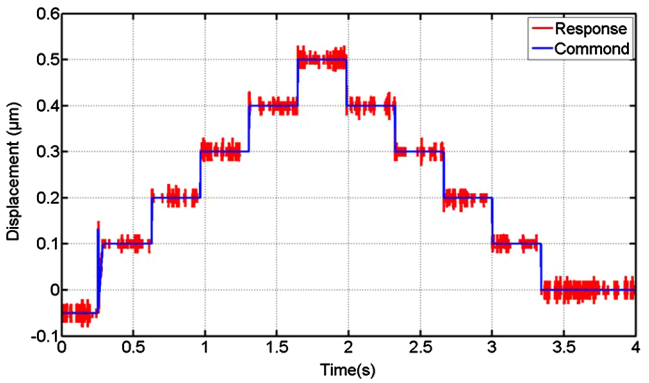

Fig. 10 The resolution of the new FTS.

sensor and the D/A converter, the electromagnetic interference during the signal transmission and processing, especially the bonding strength of the assembled parts. A stair control signal is applied to the FTS, and the displacement is recorded by the linear encoder, as shown in Fig. 10. Obviously, system noise is up to 40 nm larger than environment noise, and the motion resolution is raised to 0.1 μm. It is difficult to obtain higher machining accuracy than this value. However, several studies introduced FTS machined surfaces, and measurement results show submicron form errors. Kim et al. fabricated a copper freeform mirror of diameter 50 mm with a form accuracy of 0.15 μm after corrective figuring with on-machine measurement by a piezoelectric actuated FTS.[20] Scheiding et al. fabricated a micro-optical lens array on a steep curved substrate by use of a voice coil FTS; the measured shape error is 1.37 μm (rms).[17] That is to say, the measured motion resolution of 0.1 μm is accepted in this research.

During the diamond turning process, tool path tracking error will directly bring form error to the workpiece. The tracking performance of the new FTS must be tested. The tool paths of linear FTSs are usually approximate sinusoidal shape trajectory. Therefore, a sinusoidal wave signal is input to the amplifier of VCM. Under closed-loop control conditions, the tracking response of the FTS is shown in Fig. 11. The following error is ~0.2 μm, 0.2% of the stroke which is approximately equal to another reported VCM FTS. It can be seen that the maximum form error occurs near the mid position where FTS changes the motion direction. This is caused by the zero drift of VCM amplifier, and a high performance amplifier and controller are needed.

4 Tool Center Setting of the FTS

For the general method, a rotationally symmetric surface is usually machined first; an off-machine high-magnification microscope is used to test the workpiece for adjusting tool height. Then the form error of the surface is measured for adjusting horizontal position of tool center.[21] Bono developed several methods for tool center setting on a precision lathe and designed a flexure-based tool holder to adjust the tool center,[21–24] but it is not suitable for FTS diamond turning. Tool setters, which are usually expensive, are also used to adjust tool center. For freeform surface diamond turning, Yin et al. analyzed the form error of off-axis aspheric surface caused by tool centering error that all the three directions are error-sensitive directions.[21] It means that tool centering

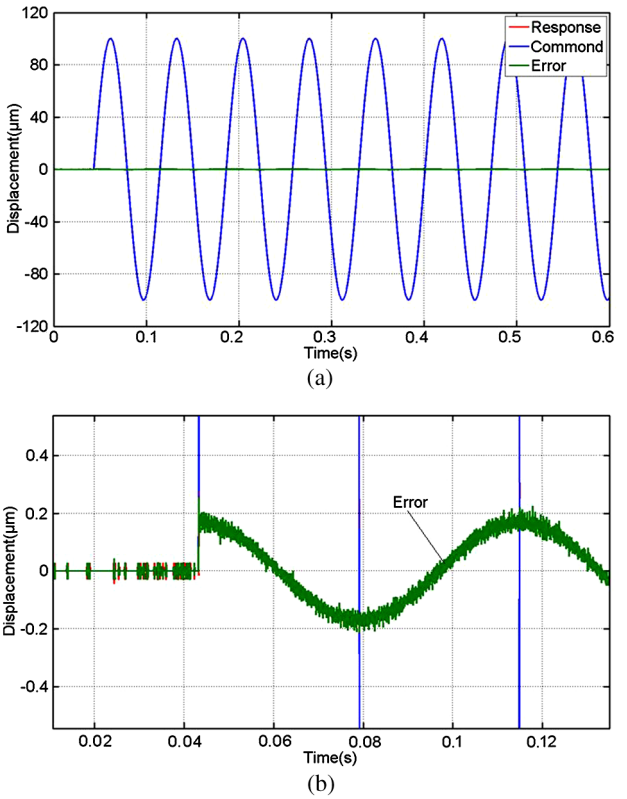

Fig. 11 Tracking performance of the FTS system. (a) Tracking performance. (b) Partial enlarged drawing.

errors in x and y direction must be eliminated. Kim et al. presented a method to compensate the tool centering error to improve the machining accuracy except the center of workpiece.[10] Therefore, the tool center position in machine tool coordinate system must be carefully adjusted while FTS is fixed on DTM. In this research, a simple and precision method is described to adjust the tool center.

4.1 *Vertical Direction Tool Center Adjustment*

The tool height is adjusted first. A flat surface is needed with a good surface finish. It would be better to cut off the power of the VCM.

First, keeping the spindle still, the slide moves along x direction, bringing the tool across the workpiece to draw a line on the surface. The schematic diagram is shown in Fig. 12. The cutting depth of the line should be as small as possible but be larger than the tool rounded edge radius and surface roughness. Next, the spindle turns 180 deg; another line is drawn. Two parallel lines are drawn on the flat surface by the diamond tool while tool geometry is duplicated on the testpieces surface. The second line can be shorter than the first line to distinguish which line is drawn first.

There are two cases of the two parallel scores as shown in Fig. 13. If the second score is higher, the result is as shown in Fig. 13(a) where the tool is higher than the workpiece center. Figure 13(b) shows that the tool is lower than spindle center. An off-machine high-magnification microscope is used to measure the distance. If the second line is above the first line, the tool center is higher than the spindle center of

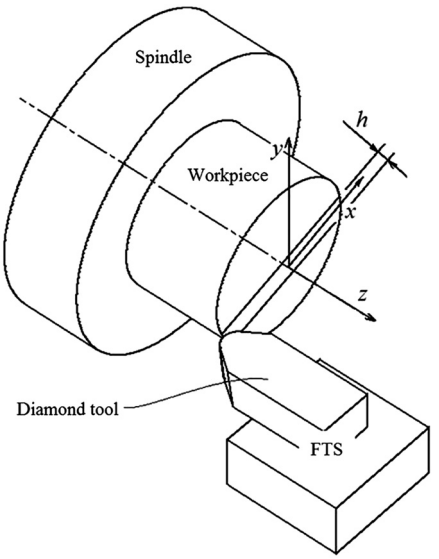

Fig. 12 The schematic diagram of the vertical direction tool center adjustment.

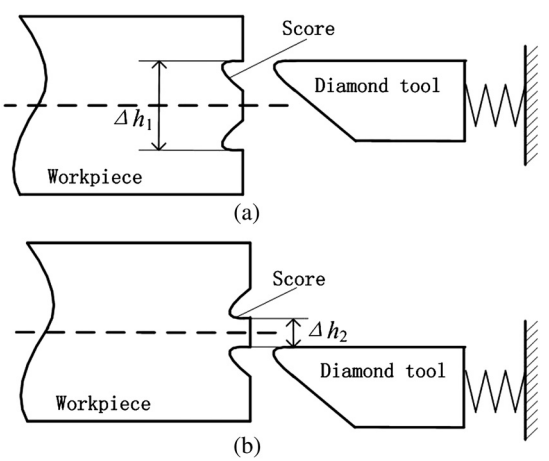

Fig. 13 Two cases of the two parallel lines.

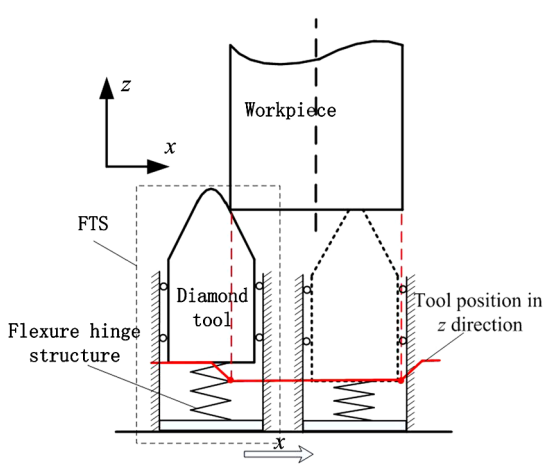

Fig. 14 The schematic diagram of the horizontal direction tool center adjustment.

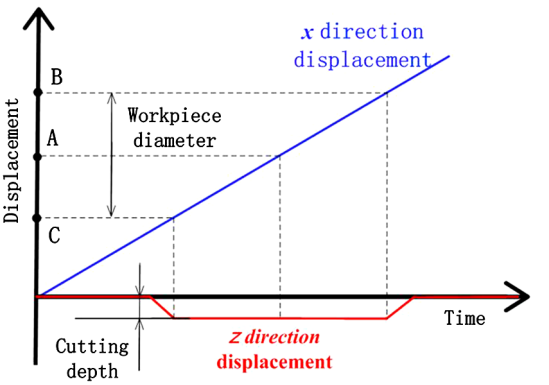

Fig. 15 Displacement changes during horizontal direction tool center adjustment.

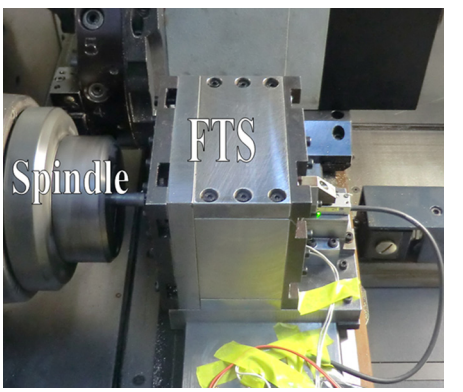

Fig. 16 FTS fixed on the diamond turning machine.

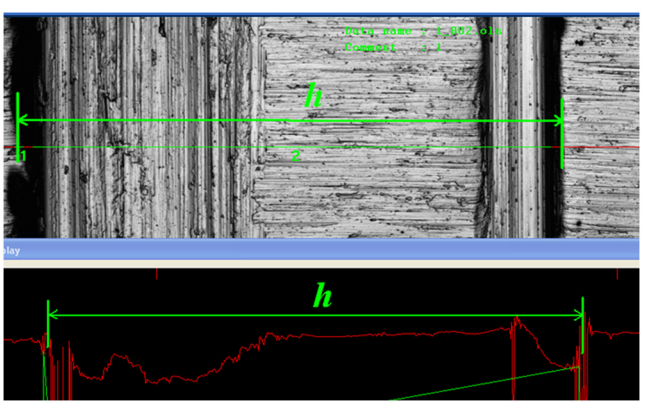

Fig. 17 The two lines for tool height adjustment.

$\Delta h_1/2$; else, the tool is lower of $\Delta h_2/2$. After that, the tool height can be adjusted with a displacement sensor.

In this method, a fine-tuning mechanism is needed to adjust the tool height. The resolution of the tuning mechanism will affect the tool height adjustment accuracy.

4.2 *Horizontal Direction Tool Center Adjustment*

The workpiece is considered to be a standard cylinder in this method, so workpiece centerline is the spindle centerline. After the tool height is adjusted, the tool center position in the machine tool coordinate system in x direction is

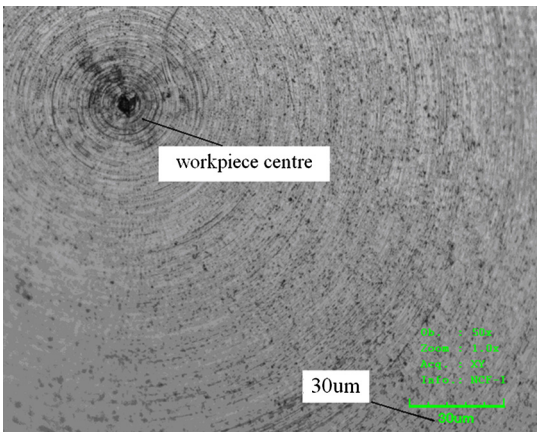

Fig. 18 Tool center error after the adjustment.

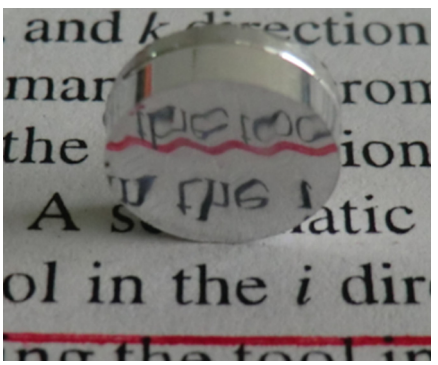

Fig. 19 The photo of the machined workpiece.

confirmed. Another line is drawn across the workpiece center. While the FTS system has only one degree of freedom, and the flexure hinge structure can be considered as an elastic mechanism; the FTS working principle can be simply described in Fig. 14.

When the tool draws across the workpiece along x direction, the tool position in z direction will be changed when the tool is contacting and leaving the workpiece. The schematic diagram of z direction tool position changes is presented in Fig. 15; the corresponding position in the x direction can be obtained, which is the point C and B. The distance between the two points is the workpiece diameter. Midpoint A is the position where the tool is just at the center of the workpiece. Then, the tool center position in x direction in the machine tool coordinate system can be obtained.

5 Cutting Experiments

The cutting experiments are carried out on a DTM. The purpose is to examine tool adjusting method and the new FTS cutting performances, such as cutting stability. The spindle is fixed on the base, and FTS is mounted on the slide, which can move along x and z directions as shown in Fig. 16. The diamond tool radius is 0.5 mm.

5.1 *Tool Center Position Adjustment*

Before the cutting experiments, the tool center must be adjusted. A flat surface was used for the tool height adjustment. As described in Sec. 4.1, two lines were drawn on the flat surface as shown in Fig. 17. According to Fig. 13, diamond tool is higher than spindle center. The distance h of the two lines was measured by OLS 3000 laser scanning confocal microscope, which is ~178 μm. Therefore, diamond tool is ~89 μm higher than spindle center.

A KEYENCE LK-G10 laser sensor with a resolution of 10 nm has been used for the tool height adjustment. A wedge mechanism has been designed to adjust the tool height, as shown in Fig. 4. The wedges were fixed at the bottom of the FTS with a slope of 100:1, which can obtain a resolution of 0.5 μm. Another advancement of the wedge mechanism is that the wedge mechanism can keep high resonance frequency of FTS pedestal. For the horizontal direction tool center adjustment, another line was drawn with tool cutting

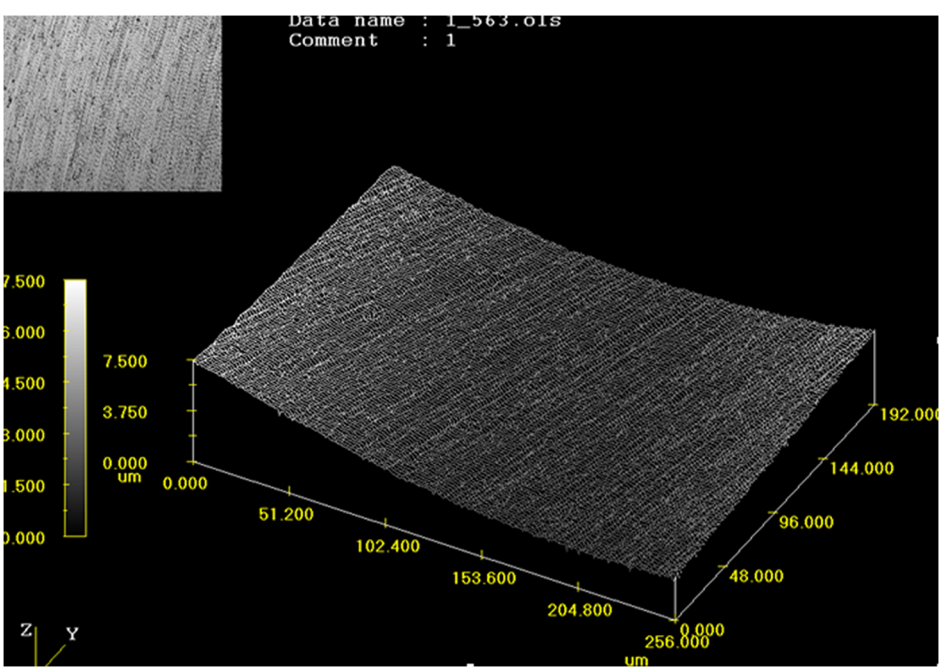

Fig. 20 Measurement result of the sinusoidal surface.

depth of 1 μm. Then, the tool center position was obtained. The workpiece machined after tool center adjustment is shown in Fig. 18. Because of the bad quality of the wedge inclined plane, the tool height error is 2.7 μm larger than ideal value of 0.5 μm.

Figure 17 shows that the workpiece material characteristics and diamond tool will affect the scores shape, which decreases the measurement accuracy of the two scores distance. In the practical applications, the optical materials have good cutting property, which is cut by high-quality diamond tools; high-precision scores can be obtained for high-accuracy tool position adjustment. Otherwise, the machining accuracy including surface roughness of the wedge mechanism affects tool position adjustment accuracy. Therefore, every part of the FTS system must be fabricated precisely.

5.2 *Sinusoidal Surface Cutting Experiments*

A 6061 aluminum part with diameter of 10 mm was used for the cutting experiments. A sinusoidal surface with five sinusoidal waves and amplitude of 20 μm is machined to certify the novel FTS system cutting performance. Tool radius compensation has been implemented in the tool path generation for the linear FTS.[25] The maximum tool cutting depth is $\sim$50 μm, and the minimum tool cutting depth is $\sim$10 μm. The part was machined at 60 rpm and feedrate of 10 μm/r. The machined workpiece is shown in Fig. 19. The surface roughness is measured by the OLS 3000 laser scanning confocal microscope, which is about Ra 26 nm, and the machined surface is shown in Fig. 20. The good sinusoidal waveform and fine machined surfaces lead us to a conclusion that this new FTS has fine cutting performance and stable working ability. In future work, the form error of the machined surfaces will be analyzed and error compensation machining technology of FTS diamond turning will be studied to obtain high-precision freeform optical surfaces.

6 Conclusion

For free-form optical surface diamond turning, a long-stroke FTS has been developed consisting of a VCM and two flexure hinges. The FTS has the advantages of high resonance frequency and high stability, with working stroke exceeding 1 mm. The resolution of the FTS is $\sim$0.1 μm and the following error is $\sim$0.2% of the full stroke. An easy and precise method, which can be used for all flexure-based FTSs, has been described to adjust the tool center position.

High-quality cutting materials and diamond tools, as well as high-precision wedge mechanisms, are needed to ensure the adjustment accuracy.

Finally, a sine wave surface has been machined. The result shows that the new FTS and the method for eliminating the tool centering error can be used in the freeform surface diamond turning.

Acknowledgments

This work was jointly supported by the National Natural Science Foundation of China (Grant No. 51175221) and the Department of Science and Technology of Jilin Province (20130522155JH).

References

1. K. Garrard et al., "Design tools for freeform optics," *Proc. SPIE* **5874**, 95–105 (2005).
2. Y. M. Sabry et al., "Silicon micromirrors with three-dimensional curvature enabling lensless efficient coupling of free-space light," *Light: Sci. Appl.* **2**, e94 (2013).
3. W Xiong et al., "Simultaneous additive and subtractive three-dimensional nanofabrication using integrated two-photon polymerization and multiphoton ablation," *Light: Sci. Appl.* **1**, e6 (2012).
4. L. D. Chiffre et al., "Surfaces in precision engineering, microengineering and nanotechnology," *CIRP Annals - Manufacturing Technology* **52**(2), 561–577 (2003).
5. E. D. Kosten et al., "Highly efficient GaAs solar cells by limiting light emission angle," *Light: Sci. Appl.* **2**, e45 (2013).
6. S. R. Patterson and E. B. Magreb, "Design and testing of a fast tool servo for diamond turning," *Int. J. Precis. Eng.* **7**(3), 123–128 (1985).
7. FTS-1000, http://www.sterlingint.com/docs/FTS-1000.pdf.
8. H. S. Kim and E. J. Kim, "Feed-forward control of the fast tool servo for real-time correction of spindle error in diamond turning of flat surfaces," *Int. J. Mach. Tools Manuf.* **43**(12), 1177–1183 (2003).
9. S. W. Gan et al., "A fine tool servo system for global position error compensation for a miniature ultra-precision lathe," *Int. J. Mach. Tools Manuf.* **47**, 1302–1310 (2007).
10. H. S. Kim et al., "Fabrication of free-form surfaces using a long stroke fast tool servo and corrective figuring with on-machine measurement," *Int. J. Mach. Tools Manuf.* **49**, 991–997 (2009).
11. S. J. Ludwick, "A rotary fast tool servo for diamond turning of asymmetric optics," Ph.D. Thesis, Massachusetts Institute of Technology (1999).
12. D. A. Chargin, "Rotary fast tool servo component design," Ph.D. Thesis, Massachusetts Institute of Technology (1999).
13. Nanotech Fast Tool Servo (NFTS-6000), http://www.nanotechsys.com/accessories/nanotech-250upl-factory-options/.
14. M. F. Byl, "Design and control of a long stroke fast tool servo," Ph.D. Thesis, Massachusetts Institute of Technology (2005).
15. S. Scheiding et al., "Freeform manufacturing of a micro optical lens array on a steep curved substrate by use of a voice coil fast tool servo," *Opt. Express* **19**(24), 23938–23951 (2011).
16. B. Nathan, "Live-axis turning," Master's Thesis, North Carolina State University (2005).
17. E. M. Zdanowicz, "Design of a fast long range actuator—FLORA II," Master's Thesis, North Carolina State University (2009).
18. S. Rakuff and J. F. Cuttino, "Design and testing of a long-range, precision fast tool servo system for diamond turning," *Int. J. Precis. Eng.* **33**, 18–25 (2009).
19. Y. J. Noh et al., "Fast positioning of cutting tool by a voice coil actuator for micro-lens fabrication," *Int. J. Autom. Technol.* **3**(3), 257–262 (2009).
20. H. Kim et al., "Fabrication of free-form surfaces using a long-stroke fast tool servo and corrective figuring with on-machine measurement," *Int. J. Mach. Tools Manuf.* **49**, 991–997 (2009).
21. Z. Q. Yin et al., "Fabrication of off-axis aspheric surface using a slow tool servo," *Int. J. Mach. Tools Manuf.* **51**, 404–410 (2011).
22. M. J. Bono and J. J. Kroll, "Tool setting on a B-axis rotary table of a precision lathe," *Int. J. Mach. Tools Manuf.* **48**, 1261–1267 (2008).
23. M. J. Bono et al., "An uncertainty analysis of tool setting methods for a precision lathe with a B-axis rotary table," *Precis. Eng.* **34**, 242–252 (2010).
24. M. J. Bono and R. Hibbard, "A flexure-based tool holder for sub-μm positioning of a single point cutting tool on a four-axis lathe," *Int. J. Precis. Eng.* **31**, 169–176 (2007).
25. X. Q. Zhou, H. Y. Zhang, and L. Ma, "The influence of process parameters on the surface topography in diamond turning of free-form optics," in *Int. Conf. on Mechanic-Automation and Control Engineering*, pp. 3480–3483, IEEE 2010).

Biographies of the authors are not available.